UNIVERSITY OF GRIEFSWALD

BACHELOR THESIS

Quasi-molecular modelling of waterdrops

Author:
Morten NAGEL

Gutachter:
Prof.Dr. Ralf SCHNEIDER
PD.Dr. Berndt BRUHN

Greifswald, July 9, 2010

Contents

1 Motivation

Why one is interested to simulate water? The answer to this question is quite obvious, due to the vital importance of water for human existence. The dominant natural source for water is rain, where raindrops [1, 2] usually hit a surface. Such an interaction of a raindrop with a surface is rather difficult to simulate resolving the full molecular complexity because of the extraordinary large number of molecules. For a mono layer of water with a radius of 0.5 cm and a molecular size of 0.305871 nm there are 10^{14} molecules in this thin layer. A spherical water drop with a radius of 0.5 cm consists of 10^{21} molecules. In addition, the dynamics of drops on surfaces is of interest, because this is needed in micro-fluid applications in biology and medicine. Here, sometimes quite surprising effects can appear, like the uphill movement of drops using resonant shaking of the surface or liquid marbles generated by addition of hydrophobic powder to the drop [3–7].

Figure 1.1: *A water drop on a leaf [8]*

For situations, where mesoscopic length scales get important, new methods are needed to allow realistic simulations of water drops and their interactions with surfaces. Microscopic systems are usually treated by Molecular Dynamics resolving the full atomistic characteristics. In contrast, macroscopic models use fluid models of Navier-Stokes equations with additional terms like surface tension. In this work, a method developed by D. Greenspan [9] is evaluated which tries to handle a waterdrop introducing a macroscopic pseudo-particle model to treat realistic sizes of waterdrops. This model is a kind of hybrid approach, because a waterdrop is described by the interaction of pseudo-particles, where one particle still contains a large number of water molecules, and the particle ensemble represents a waterdrop on a macroscopic scale with effective and simplified interaction models.

The basic goal of this work is to qualify this approach and to evaluate it with respect to computational and physics aspects, especially the physics of water drops introduced in Section 2. The basic idea of the method is presented in Section 3 , discussing especially the construction of effective potentials for the pseudo-particles. Also, a comparison with other methods, like Molecular Dynamics and Navier-Stokes fluids models is given. Afterwards, the specific numerical implementation is presented. Results for different complexity (2D, 3D) are shown in Section 5 and the validation of the method is discussed.Finally, the results of this work are summarised.

2 Basic physics of water drops

In this Section, the basic physics of water drops will be shortly introduced as needed for model validation in Section 5. The following topics are discussed

- the surface tension of a water drop
- the contact angle of a water drop with a surface

In the following a constant mass density is assumed for water, neglecting its variation with temperature

$$\rho = 1 \frac{g}{\mathrm{cm}^3}. \tag{2.1}$$

2.1 Surface tension

Surface tension is an effect of the interaction between a liquid and another material like vapour, solid or a different liquid, where the molecules of the liquid are kept together by a contracting force. This force originates from the pressure gradient between the liquid and the other material [10, 11]. Outer molecules of *e.g.* a water drop experience a force directed to the inside of the ensemble, because they are missing neighbours outside the fluid. By minimising the free energy of the system (or in other words the ratio of surface versus volume) this leads to the formation of a perfect sphere. In Tab. 1 some typical values for pure water of the nonlinear dependency of the surface tension as a function of temperature are listed. The surface tension can be reduced dramatically if small amounts of surfactants are added and can be raised if strong electrolytes are added. Therefore, measurements can vary greatly if the water is contaminated. For surface tensions between graphite and water or air no values were found. As an approximation for the graphite-air interaction the graphite-vacuum surface tension at 90 K will be used [12]:

$$\gamma_{g-a} \stackrel{!}{=} \gamma_{g-v} = 446 \frac{\mathrm{dyn}}{\mathrm{cm}} \tag{2.2}$$

$T/^\circ\mathrm{C}$	Surface Tension $\gamma/\frac{\mathrm{dyn}}{\mathrm{cm}}$
0	75.83
20	72.88
40	69.92
60	66.97
80	64.01
95	61.8

Table 1: *Surface tension as a function of temperature [13]*

2.2 Contact angle

If a drop is not only surrounded by air but also in contact with a solid, the surface tension is usually different for each interface. As a consequence a force equilibrium is established at the contact point between these three interfaces (**w**ater-**a**ir, **g**raphite-**a**ir and **g**raphite-**w**ater), which leads to a characteristic contact angle ϑ between the liquid and the solid (in air, at constant pressure). This force equilibrium is described by the Young-equation [14]

$$\gamma_{\text{g-a}} = \gamma_{\text{g-w}} + \gamma_{\text{w-a}} \cos\vartheta \tag{2.3}$$

Only, if this equation is fulfilled, the surface will not wet completely.

As the surface tensions have nonlinear temperature dependencies, this contact angle changes also with temperature due to the changed force equilibrium. The contact angle for a water drop on a flat graphite surface is [9]

$$\vartheta = 60^\circ \tag{2.4}$$

From this contact angle the height of a drop on a surface can be derived knowing the surface tension $\gamma_{\text{w-a}}$, the density ρ and the gravitational acceleration g [7]

$$h = \sqrt{\frac{2\gamma_{\text{w-a}}(1-\cos\vartheta)}{g\rho}} \tag{2.5}$$

As the surface tension is volume independent the height of a drop is it, too. Therefore, a maximum height for all water drops on a certain surface is expected. At a temperature of $293K$ this height is

$$h_{H_2O} = 0.27 \text{ cm} \tag{2.6}$$

for a water drop on a graphite surface.

3 Concept of the hybrid model

In this Section, the basic concept of the hybrid model of Greenspan [9] is presented, especially the derivation of the effective interaction potentials of the pseudo-particles.

This model aims to preserve as much as possible microscopic characteristics without the massive amount of computation power needed for full Molecular Dynamics due to the great number of molecules. Pseudo-particles are introduced, which contain a large number of water particles. To describe the behaviour of these pseudo-particles on a macroscopic scale their interactions are calculated from Mie-potentials, which need to be determined for the system studied. Extra terms for surface tension can be avoided unlike in Navier-Stokes-fluid models because this is already represented in the effective interaction potentials.

Water molecules are influenced by gravity and the interaction with other molecules. The gravitational force is the same for all molecules. The interaction force between particles is described by a kind of a Mie-potential

$$F = -\frac{G}{R^p} + \frac{H}{R^q}, \qquad G > 0, \qquad H > 0, \qquad q > p. \tag{3.1}$$

In Eq. (3.1) the first component describes the attraction and the second repulsion. For real water molecules the interaction between two molecules can be approximated by a force derived from a Lennard-Jones-potential (in dyne)

$$F(r) = (1.9646383)10^{-5}\left(12\frac{(2.725)^{12}}{r^{13}} - 6\frac{(2.725)^6}{r^7}\right). \tag{3.2}$$

Following Eq. (3.2) the equilibrium distance between two water molecules is

$$r_{eq} = 3.05871\text{Å} = 3.05871 \cdot 10^{-8}\ \text{cm} \tag{3.3}$$

D. Greenspan [9] used in his model a force with $p = 3$ and $q = 5$

$$F(R) = -\frac{G}{R^3} + \frac{H}{R^5}. \tag{3.4}$$

with the potential

$$\Phi_1 = -\frac{G}{2 \cdot R^2} + \frac{H}{4 \cdot R^4} \tag{3.5}$$

To calculate H and G, the interaction force needs to be zero between two particles at equilibrium distance. In this case the equilibrium distance of the pseudo-particles are those of molecules scaled up by a factor ν. ν is chosen with respect to numerical limits (mostly run-time limit) in the following way: for a water drop with a diameter of 1 cm and for a maximum number of about 1000 pseudo-particles in a 2D case, a ν to an $r_{\text{eq w-w}}$ in order of 10^{-2} cm is reasonable. As the equilibrium distance of water molecules in

Eq. (3.3) is of the order of 10^{-8} cm a scaling factor $\nu = 10^{-6}$ was chosen to achieve an equilibrium distance:

$$r_{\text{eq w-w}} = 0.0305871 \text{ cm} \tag{3.6}$$

which lead to

$$N = 823 \tag{3.7}$$

Therefore, one gets

$$-(0.0305871)^2 \cdot G + H = 0. \tag{3.8}$$

To determine G and H it is necessary to use a second condition, namely the total potential energy of all real molecules in the system (around $707 \cdot 10^{12}$ molecules) approximated with a (6-12) Lennard-Jones potential [9](neglecting all kinds of other energy, like kinetic, vibrational, rotational and electromagnetic):

$$\begin{aligned} E_{\text{wat.mol.}} &= 3 \cdot 707 \cdot 10^{12} \cdot 1.9646 \cdot 10^{-13} \left[\left(\frac{2.725}{3.05871} \right)^{12} - \left(\frac{2.725}{3.05871} \right)^{6} \right] \text{erg} \\ &= -104.1745 \text{ erg} \end{aligned} \tag{3.9}$$

The total energy of the system is now calculated for the total number of pseudo-particles (in this case 823) used for the simulation of the water drop [9, 15]

$$E_1 = 3 \cdot 823 \cdot \left(-\frac{G}{2 \cdot (0.0305871)^2} + \frac{H}{4 \cdot (0.0305871)^4} \right). \tag{3.10}$$

It is now assumed, that the ensemble of pseudo-particles should have the same energy [15] as the ensemble of real particles

$$\begin{aligned} E_1 &= 3 \cdot 823 \cdot \left(-\frac{G}{2 \cdot (0.0305871)^2} + \frac{4}{4 \cdot (0.0305871)^4} \right) \\ &\stackrel{!}{=} E_{\text{wat.mol.}} = -104.1745 \text{ erg} \end{aligned} \tag{3.11}$$

Together with Eqs. (3.8) and (3.11) the parameters G and H can be determined to

$$G = 1.57898 \cdot 10^{-4}, \qquad H = 1.47725 \cdot 10^{-7}. \tag{3.12}$$

Inserted in Eq. (3.5) one gets

$$\Phi_i(R) = 4\epsilon_i \left[-\left(\frac{\sigma_i}{R} \right)^2 + \left(\frac{\sigma_i}{R} \right)^4 \right]. \tag{3.13}$$

$$\epsilon_{\text{w}} = 0.0421929, \qquad \sigma_{\text{w}} = 0.0216284 = \frac{r_{eq}}{\sqrt{2}} \tag{3.14}$$

with ϵ representing the minimum energy at distance σ. Combined with Eq. (3.10) follows for the potential energy with the number of particles Eq. (3.7):

$$E_1(R) = 3 \cdot 823 \cdot 4\epsilon_i \left[-\left(\frac{\sigma_i}{R}\right)^2 + \left(\frac{\sigma_i}{R}\right)^4 \right]. \tag{3.15}$$

which results in an energy per particle in the initial state

$$E_{i(min_0)} = \Phi_{min} = 3 \cdot \epsilon_{\mathrm{w}} \tag{3.16}$$

$$= 0.128 \text{ erg} \tag{3.17}$$

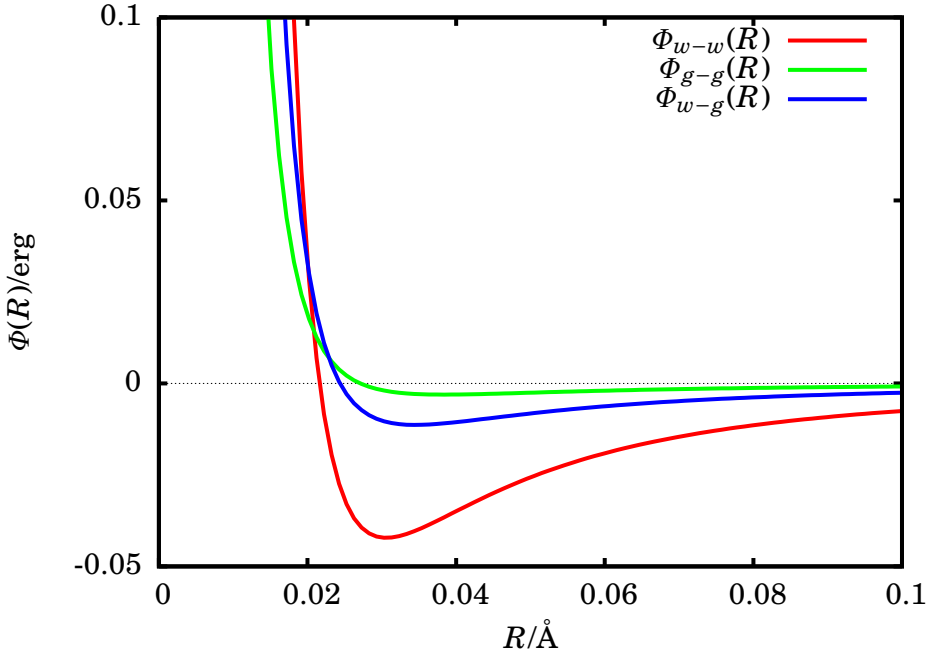

Figure 3.1: *Potentials for the different interactions*

Next the mass of each water particle needs to be calculated for the gravitational force using the mass of each water molecule

$$m = 3{,}0103 \cdot 10^{-23} \text{ g}. \tag{3.18}$$

Multiplied with the total number of molecules in the system and divided by the number of pseudo-particles, the pseudo-particle mass is given by

$$m_{\mathrm{w}} = 2.586 \cdot 10^{-11} \text{ g} \tag{3.19}$$

A similar procedure is done to obtain the potential for the interaction of two graphite pseudo-particles with a equilibrium distance of

$$r_{\text{eq g-g}} = 0.03834 \text{ cm} \tag{3.20}$$

and a mass of

$$m_g = 1.5887 \cdot 10^{-11}\ \text{g}. \tag{3.21}$$

Also, a potential like in Eq. (3.13) for the graphite - graphite interaction can be derived:

$$\epsilon_g = 3.048013 \cdot 10^{-3}, \qquad \sigma_g = 0.0271105. \tag{3.22}$$

If Eqs. (3.22) and Eq. (3.14) are combined to

$$\epsilon_{gw} = \sqrt{\epsilon_w \cdot \epsilon_g} = 0.0113404, \qquad \sigma_{gw} = \frac{1}{2}(\sigma_w + \sigma_g) = 0.02436945, \tag{3.23}$$

one gets a potential, which describes the graphite-water interaction. Finding the minimum of Eq. (3.23) the equilibrium distance between a graphite and a water particle is

$$r_{\text{eq w-g}} = 0.03446\ \text{cm}. \tag{3.24}$$

Based on the potentials, the three interaction forces are given:

$$F_{\text{w-w}}(R) = -\frac{1.579}{R^3} \cdot 10^{-5} + \frac{1.477}{R^5} \cdot 10^{-7} \tag{3.25}$$

$$F_{\text{g-g}}(R) = -\frac{1.792}{R^3} \cdot 10^{-5} + \frac{2.634}{R^5} \cdot 10^{-8} \tag{3.26}$$

$$F_{\text{w-g}}(R) = -\frac{5.388}{R^3} \cdot 10^{-5} + \frac{6.399}{R^5} \cdot 10^{-8}. \tag{3.27}$$

To obtain the equations of motions for the particles, the sum of all interaction forces and the gravitational force is calculated:

$$F_{i,\text{ges}} = m_i \cdot g + \sum_{i \neq j} F(r_{ij}) \tag{3.28}$$

As an example, one gets for a water particle i

$$M_w \frac{d^2 R_i}{dt^2} = -980 M_w + \alpha_1 \sum_j \left(-\frac{1.579}{R_{ij}^3} \cdot 10^{-5} + \frac{1.477}{R_{ij}^5} \cdot 10^{-7} \right) \tag{3.29}$$

with a scaling factor α_i for the force of interaction. To derive α_i D. Greenspan [9] uses the empirical argument that the force between two particles with a distance of five equilibrium distances away should only be a small part of the gravitational force,and suggests to use 5%. This factor and the assumed distance of interaction are important parameters determining the physics of the system as will be discussed in Section 2.
With changing the variables to

$$\bar{R} = 10R, \qquad T = 10t \tag{3.30}$$

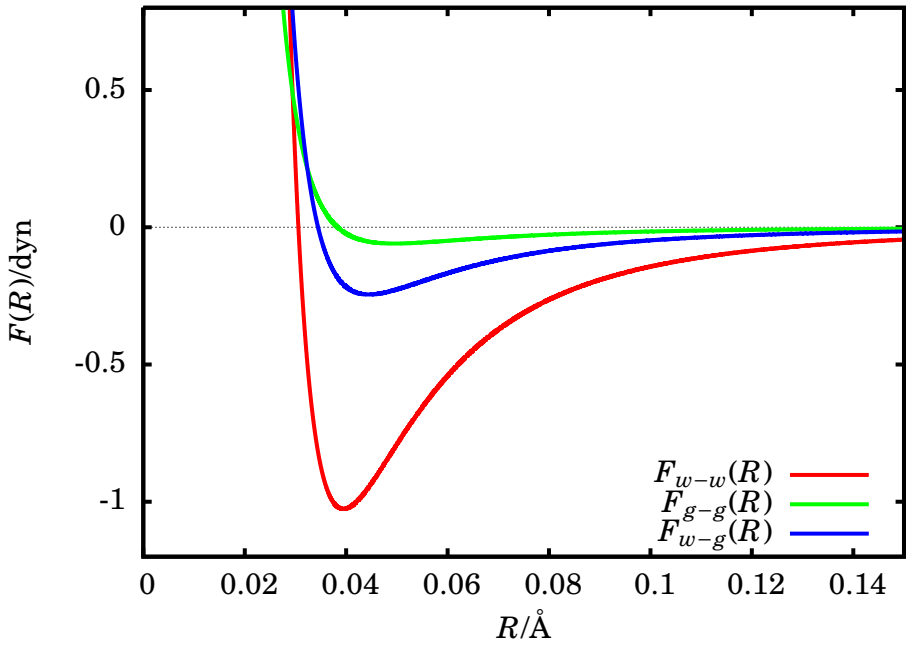

Figure 3.2: *Forces for the different interactions*

the acceleration of each water particle by water particles is

$$\frac{d^2R_i}{dT^2} = -98.0 + \sum_j \left(-\frac{18.2627}{(\bar{R}_{ij})^3} + \frac{1.70828}{(\bar{R}_{ij})^5} \right), \tag{3.31}$$

where the first term is the gravitational force. The acceleration of a graphite particle by graphite particles is

$$\frac{d^2R_i}{dT^2} = -98.0 + \sum_j \left(-\frac{35.9575}{(\bar{R}_{ij})^3} + \frac{5.285275}{(\bar{R}_{ij})^5} \right) \tag{3.32}$$

and that of a water particle by a graphite particle is

$$\frac{d^2R_i}{dT^2} = -98.0 + \sum_j \left(-\frac{26.1085}{(\bar{R}_{ij})^3} + \frac{3.10075}{(\bar{R}_{ij})^5} \right). \tag{3.33}$$

To calculate the force on a graphite particle by water, it is necessary to multiply the previous term with the factor of $\frac{m_{\text{graphite}}}{m_{\text{water}}}$ [9]. If a water particle is affected by water and graphite Eqs. (3.32) and (3.33) must be used, but counting the gravitational force only once.

4 Numerical Implementation

For the Implementation of the hybrid model presented in Section 3 a FORTRAN 90 code was written. The numerical bottleneck is the computation of the interaction of every particle with all others. This results in a size-scaling of n^2 with the number of particles n , which limits strongly the possible system sizes for this thesis. Therefore, only proof-of-principle calculations were done in 3D with about 17000 particles, and most of the work was done in 2D with up to 1000 particles.

In the following, specific details of the implementation will be presented.

4.1 Velocity-Verlet Algorithm

The integration of the equation of motion was done at every time step for every particle with the Velocity-Verlet algorithm. This algorithm consists of four steps:

1. Calculation of position by

$$\vec{x}(t+\Delta t) = \vec{x}(t) + \vec{v}(t)\cdot\Delta t + \frac{1}{2}\vec{a}(t)(\Delta t)^2 \tag{4.1}$$

2. Calculation of velocity after one half time step

$$\vec{v}\left(t+\frac{\Delta t}{2}\right) = \vec{v}(t) + \frac{\vec{a}(t)\Delta t}{2} \tag{4.2}$$

3. Calculation of acceleration $\vec{a}(t+\Delta t)$ with calculating the force F_i for every particle
4. Calculation of velocity after the full time step

$$\vec{v}(t+\Delta t) = \vec{v}\left(t+\frac{\Delta t}{2}\right) + \frac{\vec{a}(t+\Delta t)\Delta t}{2} \tag{4.3}$$

The Velocity-Verlet algorithm has the advantage of velocities and positions being time-synchronised in contrast to the half time step shifted leap frog method. As no interpolation is needed, no further error is introduced for kinetic or potential energies resulting in better stability. As a second-order method the accuracy is not as good as a higher order algorithm, like the fourth or fifth order Runge-Kutta. However, this is compensated by its lower computing cost and controlled by a small enough time step, which will be evaluated next.

4.2 Time-step

As already mentioned in Section 1 the goal of this work was to create a model which is able to describe macroscopic effects. Due to the limiting factor computing time, smaller time steps cause longer run times, as more iterations for solving the equations of motion are needed. Here, the limit of the time step is analysed.

To guarantee that a particle is interacting with the proper potential and to avoid that it will penetrate through a potential wall due to numerical errors, it is necessary to estimate the largest acceptable time step. An appropriate time step will guarantee a smoother change of the force and prohibit sudden artificial accelerations of some particles which could cause instabilities in the drop. To estimate the time step the potential Eq. (3.13) for the interaction of two particles is expanded in a Taylor series near the potential minimum at $r = \sigma_{\mathrm{w}}$ with

$$\nabla \cdot \Phi_{\mathrm{w}}(r_{\text{eq w-w}}) = \frac{\partial \Phi_{\mathrm{w}}(r_{\text{eq w-w}})}{\partial r} = -F(r_{\text{eq w-w}}) = 0 \tag{4.4}$$

to

$$\Phi_{\mathrm{w}}(r) = 4\epsilon_i \left[-\left(\frac{\sigma_i}{r}\right)^2 + \left(\frac{\sigma_i}{r}\right)^4 \right] \tag{4.5}$$

$$\begin{aligned} &= \Phi_{\mathrm{w}}(r_{\text{eq w-w}}) + \frac{\partial \Phi_{\mathrm{w}}(r_{eqw-w})}{\partial r} \cdot (r - r_{\text{eq w-w}}) \\ &\quad + \frac{1}{2} \cdot \frac{\partial^2 \Phi_{\mathrm{w}}(r_{eqw-w})}{\partial r^2} \cdot (r - r_{\text{eq w-w}})^2 + O(r^3) \end{aligned} \tag{4.6}$$

$$= -\epsilon_{\mathrm{w}} + 4 \cdot \epsilon_{\mathrm{w}} \left[-\frac{6 \cdot \sigma_{\mathrm{w}}^2}{r_{\text{eq w-w}}^4} + \frac{20 \cdot \sigma_{\mathrm{w}}^4}{r_{eqw-w}^6} \right] \cdot (r - r_{\text{eq w-w}})^2 \tag{4.7}$$

$$= -\epsilon_{\mathrm{w}} + \frac{1}{2} \cdot \frac{4 \cdot \epsilon_{\mathrm{w}}}{\sigma_{\mathrm{w}}^2} \cdot (r - r_{\text{eq w-w}})^2 \tag{4.8}$$

The result is a harmonic oscillator potential:

$$\Phi(r) = V_0 + \frac{m \cdot \omega^2}{2} \cdot (r - r_{eqw-w})^2 \tag{4.9}$$

The coefficients gives the frequency or with $\tau = \frac{2 \cdot \pi}{\omega}$ the period of the oscillation for two water particles.

$$\tau_{w-w} = \pi \cdot \sqrt{\frac{m \cdot \sigma_{\mathrm{w}}^2}{\epsilon_{\mathrm{w}}}} = 1{,}6822 \cdot 10^{-6} \text{ s.} \tag{4.10}$$

To resolve the movement of the pseudo-particles one needs to choose a time step at least 10 times smaller then this period. For the interaction of a graphite and a water particle a time step of

$$\tau_{w-g} = 3{,}6896 \cdot 10^{-6} \text{ s} \tag{4.11}$$

is needed. The time step for the calculations in this work was chosen in the range between $\tau = 5 \cdot 10^{-7}$ to $1 \cdot 10^{-8}$ s. D. Greenspan chose a much larger time step of $\tau = 5 \cdot 10^{-}5$ s [9] well beyond this limit, which obviously can cause artificial results. Such a time step can lead to results where the drop is unstable and sometimes looses some particles. Also the interaction with the surface is not correctly resolved and the

drop can penetrate the surface without resistance. Therefore, even if a physically plausible result is observed at the end of a calculation, if the time step is chosen too large, its interpretation is uncertain due to numerical errors. The same is true, if particles have too large kinetic energies as a too fast particle may also not experiences the correct interaction, because its larger velocity requires shorter time steps. Therefore, a limitation of the kinetic energy is needed, introduced by damping in this model.

4.3 Damping

Damping is needed for different reasons. As a thermal temperature is not existing in the model, viscous damping of the velocities is used to relax to reasonable steady-state conditions. Some particles can gain energy due to numerical errors, although no force is existing. Again, damping is needed to stabilise the numerics. Also, oscillations around an equilibrium state can be avoided by moderate damping to obtain equilibrium states.

To save computing time the damping is not calculated individually for each particle as a viscous force depending nonlinear on its velocity or the difference of velocity to its neighbours. Instead, a constant re-scaling factor less than one is multiplied after a given number of time steps to all velocities. After applying the viscous damping spikes appeared in $(\Delta r)^2$ and $(\Delta v)^2$, because positions and velocities are no longer consistent and produced therefore transiently large numerical accelerations. Variation of the damping shows that the final results are independent from this damping factor, if it is above a certain level and avoids numerical errors due to too high velocities. In fact, a stronger damping caused only a longer run time, as the damping limits the maximum of kinetic energy and so the maximum velocity of a falling drop onto the surface as the equilibration time needed. An example of the influence of too high kinetic energy is a collision of drops. Here, if the initial velocity is chosen too large, the collision leads to the creation of a large number of smaller drops (see Fig. 4.1).

4.4 Initial conditions

Damping is also used for the initialisation of water drops. For this, the particles are chosen on a cube with random velocities. Then, this system is equilibrated until a sphere is formed and the initial velocities are damped to zero. For the simulation of a falling drop, the drop centre is positioned above the middle of the plate.

The creation of a graphite plate as a surface, which the drop hits, is more complicated. Here, one has to avoid the natural tendency of the graphite particles to equilibrate a sphere. Different approaches were tested: one with mirroring the particles at the defined boundaries or one using static particles defining the plate boundaries. One result is shown in Fig. 4.2. Here, several layers of fixed particles were used and additional free-moving graphite particles were put on top. However, these formed a contracted cluster, destroying the initial plate configuration.

In the end, also for reducing the computational costs considerably, all graphite particles are considered as static.

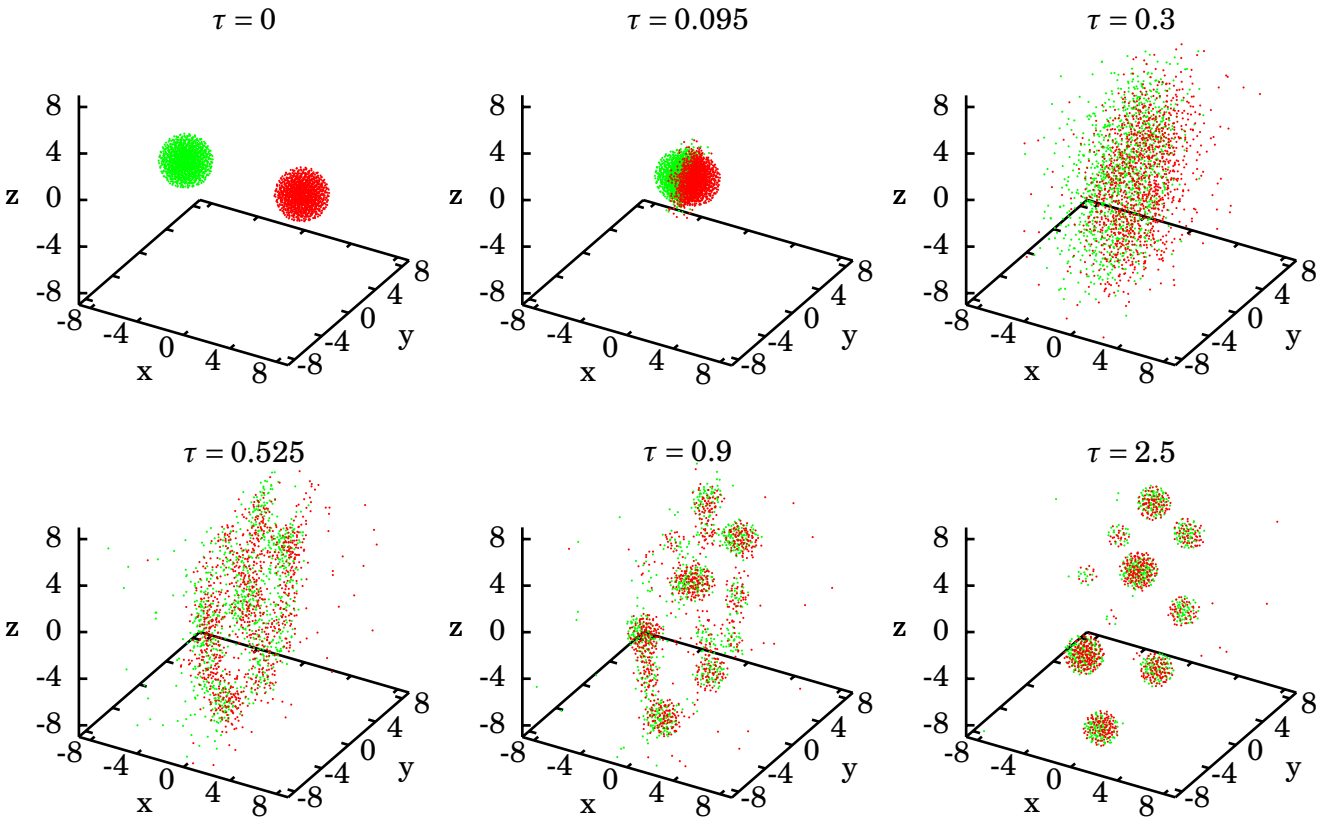

Figure 4.1: *Collision of two water drops with large velocities, which caused a splitting into smaller droplets*

To initiate a specific configuration a control tool was written, which allows to move, add, rotate or sort the particles. With this tool and additional scripts a start ensemble like a drop above a skew plate can be created easily.

4.5 Run-time optimisation

As mentioned before the large computational times needed for one calculation limits the work in this thesis. One 3D calculation [16–18] with adequate time steps would have last 400 days. Therefore, 2D calculations are used with a final run-time of 25 hours for each case. To shorten the run-time the maximum time step still giving acceptable numerical and physical results (as discussed before) has to be chosen. Also, the total simulated time for each case is taken as small as possible and the dominant subroutine, namely the calculation of the force, is optimised. The different optimisation measures are discussed in the following.

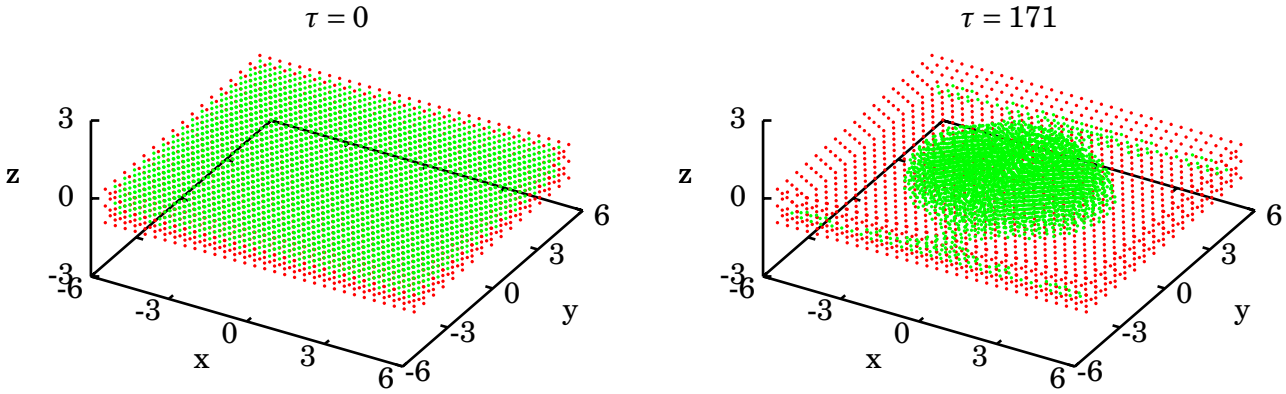

Figure 4.2: *Agglomeration of graphite particles in the centre of same layers of predefined static particles*

4.5.1 Maximum distance of interaction

A simple optimisation is possible based on the fact that potential Eq. (3.13) and the force Eq. (3.25) approaches zero, if the distance between two particles is getting large:

$$r \to \infty \Rightarrow \begin{matrix} \Phi(r) \to 0 \\ F(r) \to 0 \end{matrix}. \tag{4.12}$$

Assuming that the total force acting on one particle can be approximated by the sum of forces up to a certain distance particle interactions are considered only within this cut-off distance neglecting all interactions with more distant particles. As will be shown later, results varies strongly with changes in this cut-off distance.

4.5.2 Link-list

A further optimisation step is to introduce a link list as known from Molecular Dynamics, because for the calculation of the interaction forces the actual distance has to be compared with the cut-off distance, which is computationally expensive. In the link list the neighbours within this cut-off distance of one particle are listed and it is no longer necessary to check every force calculation if two particles are close enough to interact. The link list is updated every tenth step accepting a small error if a particle left or entered the sphere of interaction between two list calculations.

Due to different interaction of a water particle with graphite or another water particle, the link list is split up into a water-water and water-graphite interaction part. By this, a check of the interaction type can be avoided. Also, the arrays of positions, velocities and forces are sorted before this to avoid checks for static particles. The sorting of particles with respect to their horizontal positions was tested to allow for faster determination of neighbours. However, at the end, this procedure is not used, because the sorting needs a

lot of computing time and an algorithm to map an array position to the particle position was not available.

4.5.3 Dynamic adaption of base plate

To save computing time it is also necessary to adapt the graphite plate size dynamically. This was needed to avoid artifacts of a too small plate resulting in possible too small drops or even worse a loss of particles over the plate edges. On the other hand, a too large plate requires many particles, resulting in a longer computing time. As the maximum distance of interaction is given through Subsection 4.5.1 the plate is adapted dynamically after a certain time with an edge length larger than the diameter of the water drop extended to the double length of the interaction distance.

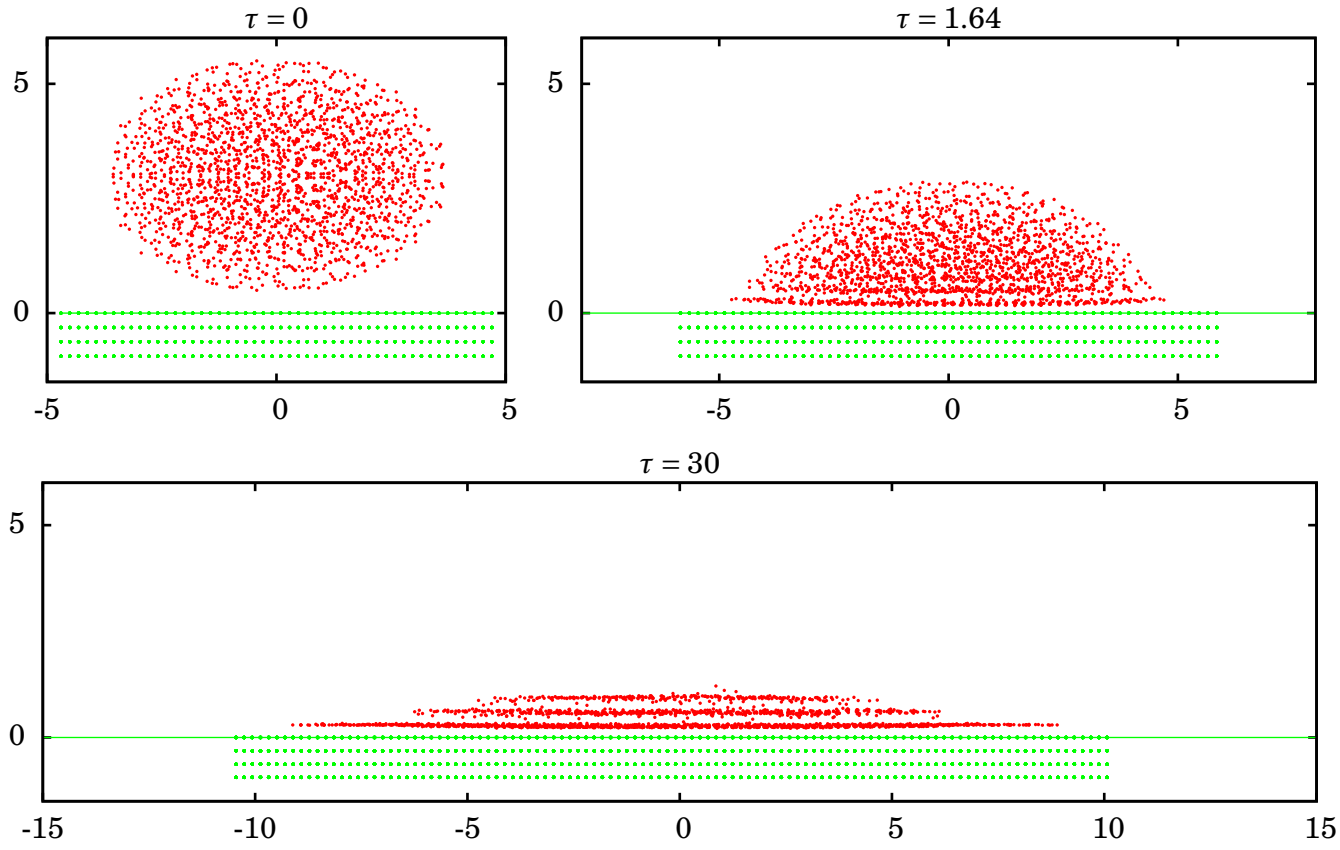

Figure 4.3: *Expansion of the graphite plate due to extension of the water drop*

5 Model validation and results

In the following results of the code implementing the hybrid concept will be presented and a validation of the hybrid concept will be done. Each run is started with an equilibrated drop as described in Section 4 (see Fig. 5.1). The cases differ by their initial velocity, the number of particles and mainly their different distances of interaction.

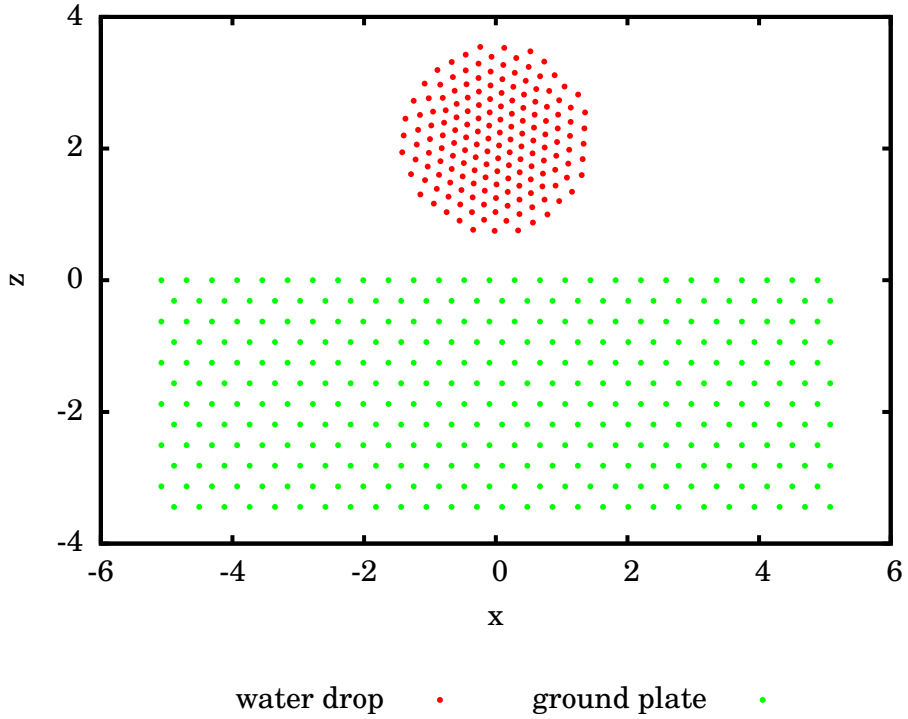

Figure 5.1: *A typical start with a water drop of* 168 *particles,* 324 *graphite surface particles and a distance of interaction* $r_c = 10 \cdot r_{eq\ w\text{-}w}$ *- all axes in this and following figures are in mm unless explicit remarked*

5.1 Distance of interaction

The interaction distance r_c is the main variation parameter as the parameters for the potential and the force were taken constant. Increasing this distance the particles are pushed closer to each other as more and more particles act attractive. As a consequence the diameter of the start drop and the surface of a drop on the base surface was reduced seen as in Fig. 5.2. A larger interaction distance results unfortunately in much higher computational costs.

In Fig. 5.3 the pair-distribution function of the distance between two water particles in the equilibrium state before and after the drop on the surface is analysed. The cut-off distance $r_c = 10 r_{\text{eq w-w}} = 3.059$ cm is so big, that nearly all particles interact with each

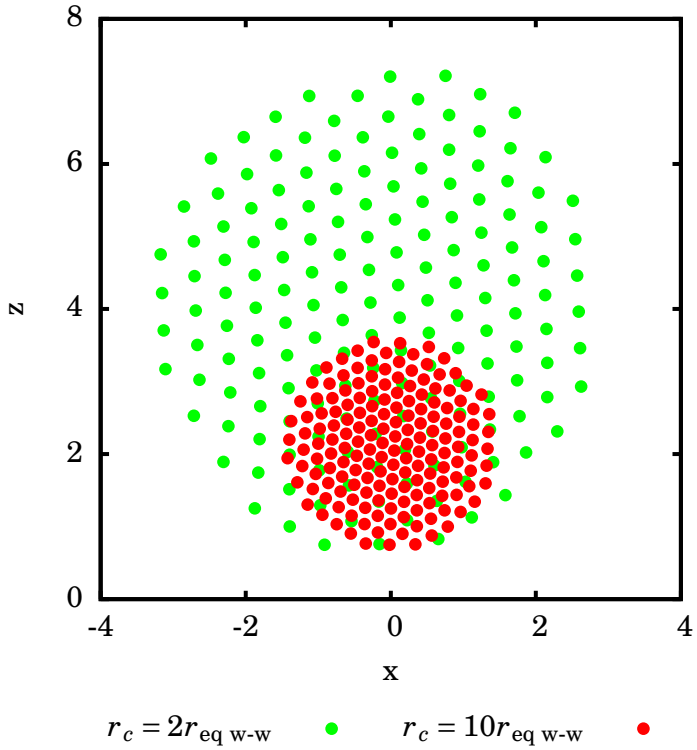

Figure 5.2: *Comparison of drops with the same number of particles but different interaction distances*

other, especially in the situation before the drop as the furthest distance are smaller then r_c. Moreover an internal structure of the drop is visible as the distribution is in some kind discrete as also seen in Fig. 4.3. Furthermore in the distribution after the drop the influence of the graphite surface is quiet viable, as on the one hand due to the not longer perfectly spherical shape there are more further connections and on the other hand due to the attractive force of the plate all particles are closer together causing a shift of the distribution peaks in contrast to the distribution before the drop.

Form Fig. 5.3 also the shrinking of the drop diameter can be qualified, as the smallest distance is the real equilibrium distances r_{ik}. In contrast to the assumed equilibrium distance from Eq. (3.6) in the model, one gets

$$r_{ik} \approx \frac{2}{3} r_{\text{eq w-w}} \approx \sigma_{\text{w}} \approx 0.21 \text{ cm}. \tag{5.1}$$

If the radius of a sphere shrinks by this factor $\nu = \frac{2}{3}$ its volume is also at least reduced to one half, if it is a two dimensional object, or in case of three dimensional object to one third, which leads to a density different from Eq. (2.1). This has a serious impact, because the forces (3.31), (3.32) and (3.33) are standardised in Eq. (3.29) with the from the start volume derived masses. And as only the drop is contracting and not the static surface the force equilibrium of surface tensions in Eq. (2.3) is disturbed, which will result in a modified contact angle.

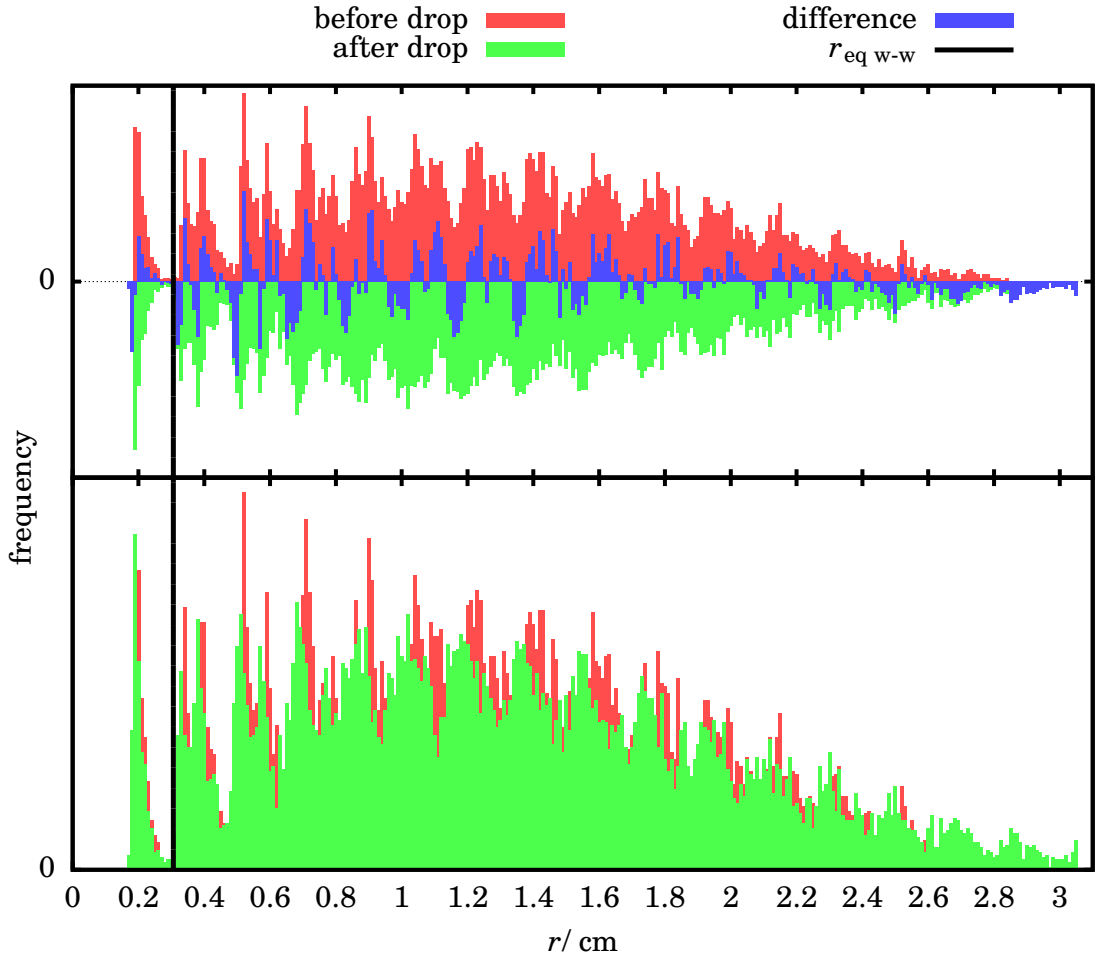

Figure 5.3: *Pair -Distribution function of distance between two particles*

5.2 Contact angle

The area of the surface decreases as the distance of interaction is increased. Therefore, the contact angle between the drop and the surface must also raise. From Subsection 2.2 a contact angle of $\vartheta = 60°$ is excepted and can be achieved with a large distance of interaction as shown in Fig. 5.4. Because the number of particles used for the calculation is rather small, one particle more or less at the periphery of the drop can make a difference of 20°. A quantitative validation of the results is not possible due to these large statistical variations.

The contact angle is also tested with a flow of a drop over a skew surface, where the drop follows the gravitational force and finally drops off the plate. The results are shown in Fig. 5.5, where an ellipsoidal drop hits a skew surface. At the time $\tau = 1.0$ the contact angles at the front and the back are nearly the same and the drop has not the expected shape of a downhill moving drop with a greater contact angle at the front compared to the one at the back.

Both results demonstrates that the surface tension is not reproduced correctly within

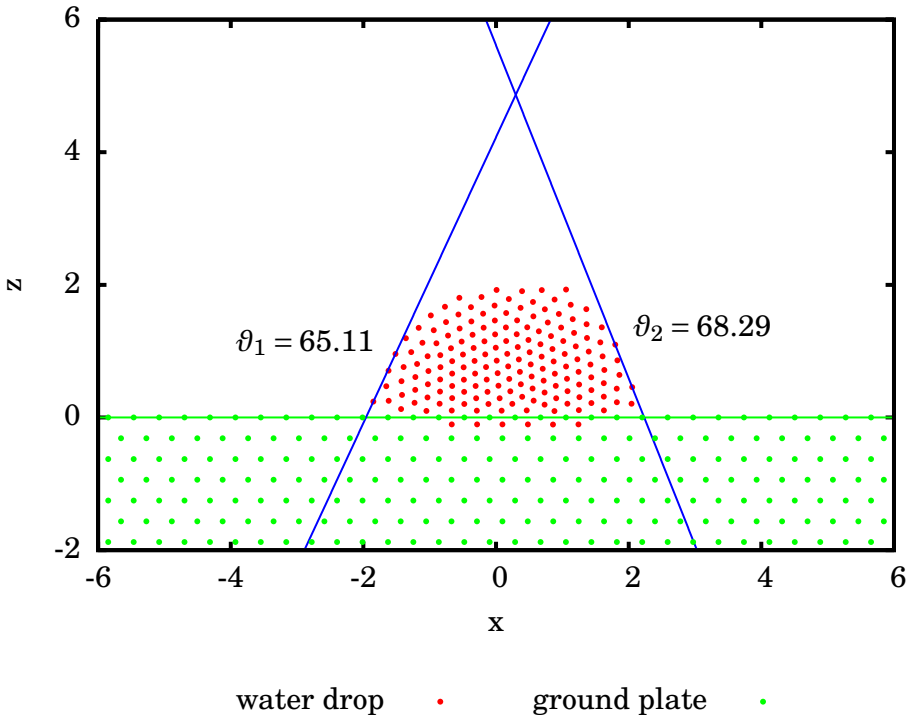

Figure 5.4: *An equilibrated drop on a surface*

the model.

5.3 Separation from a top plate

A test for the force between drop and surface is done in the following way: If the ensemble of an equilibrated drop on the surface is turned upside down, the separation from a top plate through the gravitational force like in [19] is simulated. In Fig. 5.6 the strength of the gravitational force had to be increased by two and a half times. This result indicates a far too strong force between the surface of the plate and the water drop.

5.4 Diffusion of particles into the surface

A too large time step (see Subsection 4.2) can cause artificial results like diffusion of particles into the plate. For too high initial velocities and weak damping the particles are oscillating heavily and the particles do not experience the full repulsive potential of the surface particles due to time step limits. In cases of too large distances of interaction the particles get too close, while the surface particles are static as seen in Section 5.1. The diffusion now occurs because the large number of particles on top of the drop are also attracted by the surface particles and push the fewer particles in the direct

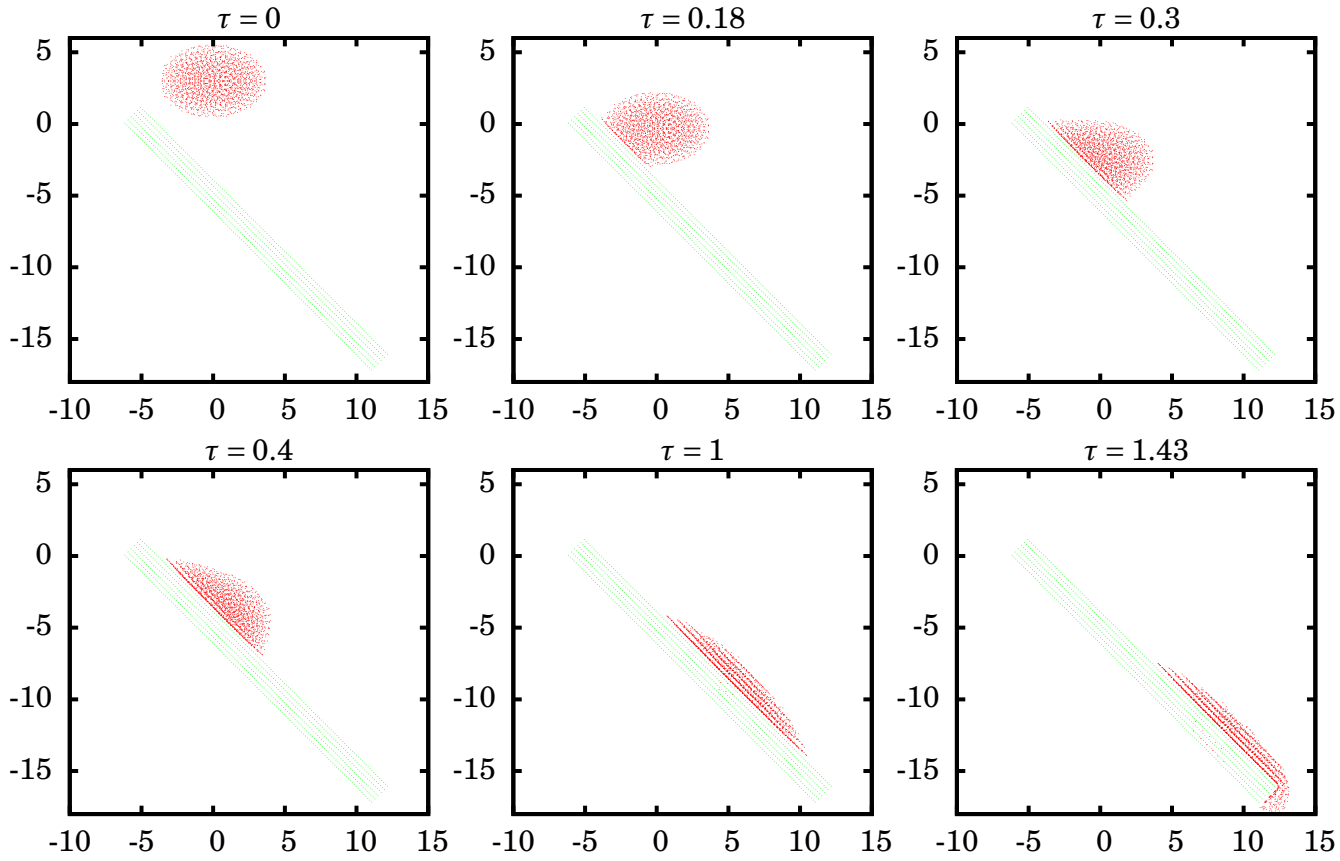

Figure 5.5: *A drop moving over a around 45° skewed plate due to the gravitational force. The plate is not big enough for the whole drop which causes floating over the edges*

neighbourhood of the graphite into the surface. Following this a shorter distance of interaction would be recommended, but as shown in Subsection 5.2 this does not result in a correct contact angle leading to a contradiction in the model parameters.

5.5 Validation of the surface tension

Because surface tensions are macroscopic effects, the direct validation in the model is difficult. As already mentioned in Subsection 2.1 a pressure gradient is not existing in this model, therefore the surface tension between water and air can not be calculated directly. Also, the temperature dependence can not be checked as in the model a temperature is not defined. Additionally, as shown later in Subsection 5.6, the force is normalised to the total mass of the particles, but effects of the surface tension like the contact angle to other materials are mass-independent. Due to this normalisation to the particle mass the strength of the interaction force between water particles and between water and graphite particles are nearly the same. If the results from the previous Subsections are considered, the surface tension between the solid graphite plate

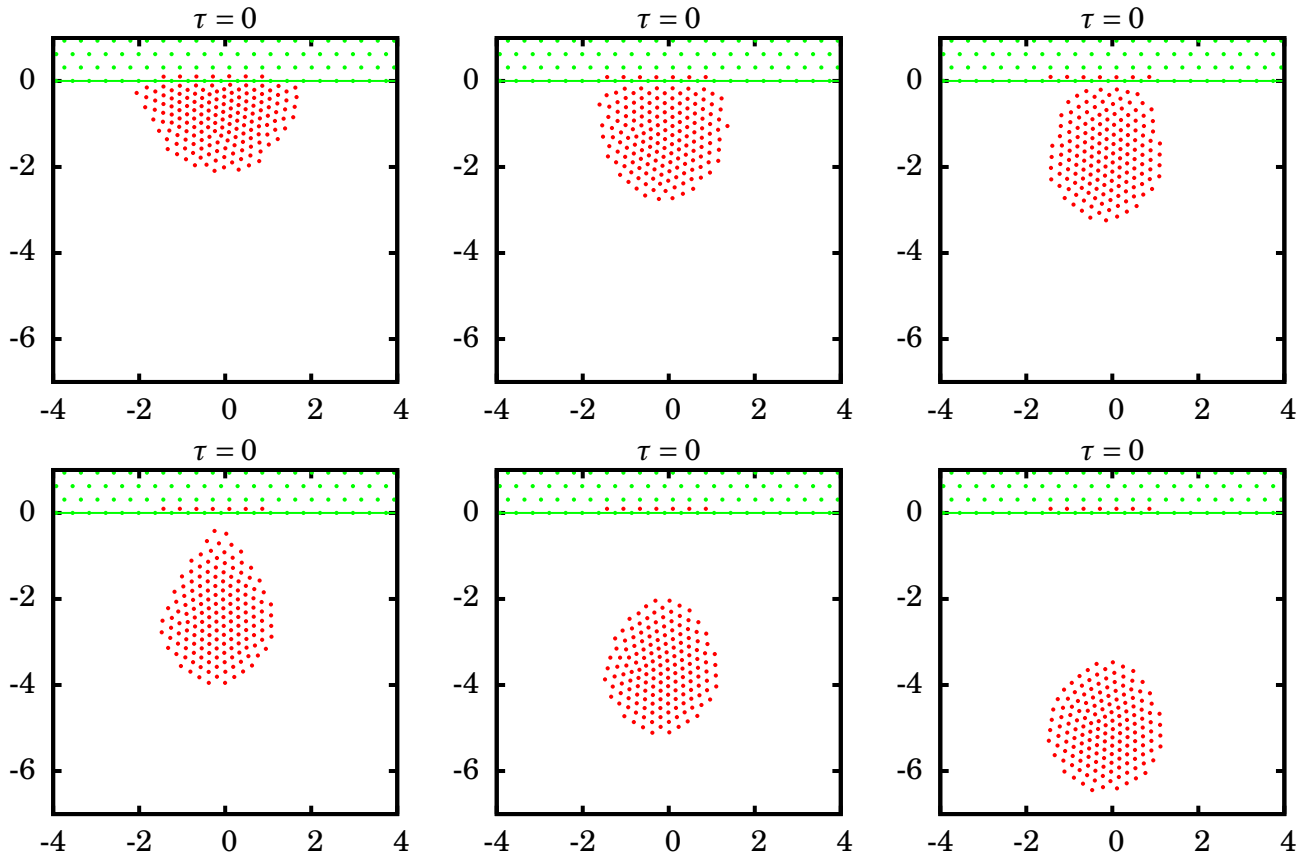

Figure 5.6: *Sequence of a separating water drop*

and the water drop seems to be too strong. Using Eqs. (2.2),(2.3) and (2.4) the expected surface tension for the graphite-water interaction is

$$\gamma_{g-w} = \gamma_{g-a} - \gamma_{w-a}\cos\vartheta \tag{5.2}$$

$$= 408.5\frac{\text{dyn}}{\text{cm}} \tag{5.3}$$

In the following an estimate is presented, if the model attraction forces between particles are used to calculate the surface tension between water and air. From the simulation (as seen in Fig. 5.3) the distance of nearest neighbours is approximately given by Eq. (5.1). If the particle i is a particle at the surface and particle k its direct neighbour, that in equilibrium state without gravity

$$F_{i,ges} = \sum_{j\neq i} F(r_{ij}) = 0. \tag{5.4}$$

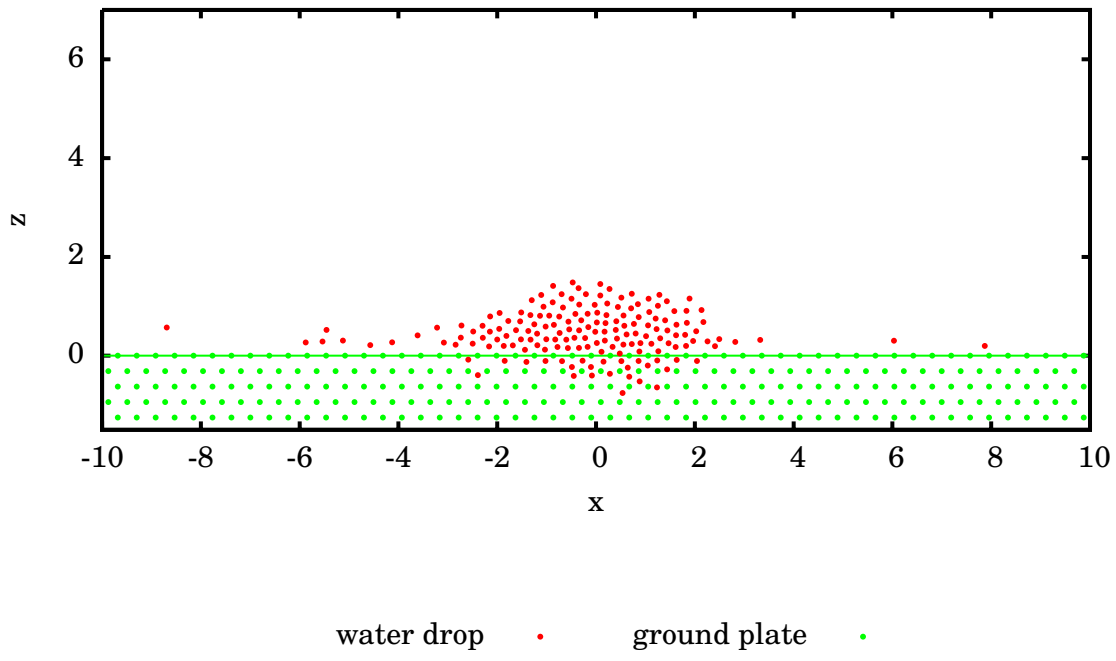

Figure 5.7: *Result of an impact of an unstable drop with large time-step* $\Delta t = 5 \cdot 10^{-5}$ *and a large distance of interaction* $r_c = 10 r_{eq\ w\text{-}w}$

As $F(r_{ik})$ is the only repulsive force, this leads to

$$F(r_{ik}) = \sum_{j \neq i,k} F(r_{ij}) \tag{5.5}$$

$$= -\frac{1.579}{r_{ik}^3} \cdot 10^{-5} + \frac{1.477}{r_{ik}^5} \cdot 10^{-7}. \tag{5.6}$$

The surface tension is approximated by

$$\gamma_{w_a} = \frac{\partial F_{i,ges}}{\partial r}. \tag{5.7}$$

$\frac{\partial F(r_{i,k})}{\partial r}$ is in γ_{w_a} the dominating part as $\left(\frac{\partial F(r_{i,k})}{\partial r} \approx 2.5 \cdot 10^2 \cdot \frac{\partial F(2 \cdot r_{i,k})}{\partial r}\right)$. This leads to

$$\gamma_{w_a} \approx \alpha_1 \left(\frac{3 \cdot 1.579}{r_{ik}^4} \cdot 10^{-5} - \frac{5 \cdot 1.477}{r_{ik}^6} \cdot 10^{-7} \right) \tag{5.8}$$

which leads finally to a surface tension of

$$\gamma_{w_a} = 0.151 \frac{\text{dyn}}{\text{cm}} \tag{5.9}$$

which is a factor of $\nu = 5 \cdot 10^2$ too small. As a summary, one gets rather contradicting results for surface tension: the surface tension between graphite and the water drop is too large, whereas the surface tension between water and air is far too small.

5.6 Energy

The total potential energy of the system is needed to calculate the Mie-potentials for the interaction of particles. As shown in Section 3 this energy is derived from the potential energy of an ensemble of water molecules ordered in a thin layer with the classic Lennard-Jones potential. This calculation suffers from three shortcomings

- as a polar fluid the calculation with a Stockmayer Potential would be more accurate
- only the potential energy between direct neighbours was considered
- there exists better potential data [20]

The restriction to only nearest-neighbour interactions is also posing problems for the construction of the energy for the particle interaction. In case of considering only nearest neighbour interactions for the water molecules calculated with the Lennard-Jones-potential the energy

$$E = 110.63 \text{ erg} \tag{5.10}$$

is only $\approx 7\%$ larger than the value calculated in Eq. (3.9). On the other hand for the particle interaction Eq. (3.15) considering 2 equilibrium distances one gets:

$$\Phi_{min} = 3 \cdot 4\epsilon_\text{w} \left[-\left(\frac{\sigma_\text{w}}{r_\text{eq w-w}} \right)^2 + \left(\frac{\sigma_\text{w}}{r_\text{eq w-w}} \right)^4 \right] + 6 \cdot 4\epsilon_\text{w} \left[-\left(\frac{\sigma_\text{w}}{2 \cdot r_\text{eq w-w}} \right)^2 + \left(\frac{\sigma_\text{w}}{2 \cdot r_\text{eq w-w}} \right)^4 \right]. \tag{5.11}$$

With Eq. (3.14) follows

$$\Phi_{min} = 3 \cdot \epsilon_\text{w} \left[-1 + 8 \left(-\frac{1}{8} + \frac{1}{64} \right) \right] \approx -6\epsilon_\text{w} \tag{5.12}$$

$$\approx -0.258 \text{ erg} \tag{5.13}$$

which is nearly twice as much as in Eq. (3.17). This error introduced by the initial assumption is after all quite big. In addition, the results of Subsection 5.1 showed also that the ensemble of particles is not in its potential minimum introducing an additional error for all energy calculations. If in Eq. (3.9) the energy minimum is not used in the model all parameters get rather arbitrary and the link to the microscopic model is lost.

This energy normalisation seems also unnecessary, as the potential is defined completely by the determination of the equilibrium distance $r_\text{eq w-w}$ between two particles. Using this distance between particles the number of particles per volume can be estimated and with the constant density (2.1) the mass of each particle M_w follows. The potential is independent from a specific system and its specific volume and mass, because the normalisation of energy done in Eq. (3.11) can also be derived without knowing the exact number of molecules N_{mol} in the observed system from Eq. (3.9):

$$E = 3 \cdot N_{mol} \cdot E_\text{pot.min.mol} \tag{5.14}$$

$$= 3 \cdot \frac{M_\text{ges}}{M_{mol}} \cdot E_{pot.min.mol} \approx M_\text{ges} \cdot -4.8904 \cdot 10^9 \frac{\text{erg}}{\text{g}} \tag{5.15}$$

where $E_{\text{pot.min.mol}}$ is the potential minimum, when two molecules are at equilibrium distance and M_{mol} is the mass of a molecule. If the particles are predefined with a certain mass like $M_{\text{w}} = 2.586 \cdot 10^{-11}$, from Eq. (5.14) the whole potential can be derived using the number of particles Eq. (3.7)

$$\epsilon_{\text{w}} = \frac{E}{3 \cdot N} \approx \frac{E}{3 \cdot \frac{M_{\text{ges}}}{M_{\text{w}}}} \overset{(5.15)}{=} \frac{m_{\text{w}} \cdot 4.8904 \cdot 10^{9} \frac{erg}{g}}{3} \tag{5.16}$$

$$\approx 0.4215 \text{ erg} \tag{5.17}$$

which differs only slightly from Eq. (3.14), but is completely independent from the size of the drop. Also, ϵ_{w} is only an additional multiplicative factor and is nullified by α_i in Eq. (3.29) normalised to the gravitational force of the particle mass, and due to this also defined by the equilibrium distance.

Instead of applying a normalisation to particle mass, a normalisation to the inner energy could be done. One possible way, using a physics-based procedure, could be to determine the potential minimum with the energy needed to evaporate all water of the drop with a mass

$$M_{\text{ges}} = 823 \cdot M_{\text{w}} = 823 \cdot 2.586 \cdot 10^{-11} = 2.128 \cdot 10^{-8} \text{ g}. \tag{5.18}$$

Zero kinetic energy is used in the model, even water is considered at a pressure of 1 atm. For $T_0 = 273K$, the melting temperature for water, the enthalpy of vaporisation is $\Delta H_v(T_0 \rightarrow 373K) = 45,054 \frac{kJ}{mol}$ [21]. It follows with a molar mass of water $M = 18.02 \frac{g}{mol}$ an energy

$$E_{\text{enthal.}} = \frac{\Delta H_v}{M} \cdot M_{\text{ges}} = 532.116 \text{ erg} \tag{5.19}$$

is needed to vaporise a mass M_{ges} of water with T_0. Comparing with Eq. (3.9), this energy is higher and so a water drop in the hybrid model vaporise much earlier than in reality.

Although this procedure seems rather viable, certain problems prevent its direct application. During the phase transition the correlation between inner energy and temperature is really nonlinear and also a link between temperature and kinetic energy of the particles was not established through normalisation. Also, in the hybrid scheme due to damping and the scaling of the gravitational force energy conservation is not given. If the model could be reformulated guaranteeing energy conservation, the problem still remain that, if a particle would vaporise and leave the ensemble, the mass loss would not appear in a continuous form but as statistical events, which could cause numerical instability problems.

5.7 Additional results

An additional scenario was investigated with this model, namely the flow of a water drop through a capillary. To achieve this, after equilibrating a drop on the surface a channel of base plate particles was removed, so that the drop could move due the gravitational force in this channel as seen in Fig. 5.8. As discussed before in Subsection 5.2, the contact angle in this case between drop an capillary is also rather uncertain, because the movement or displacement of one particle changes it by a large amount. Not surprising is the velocity in the centre higher as at the boundaries.

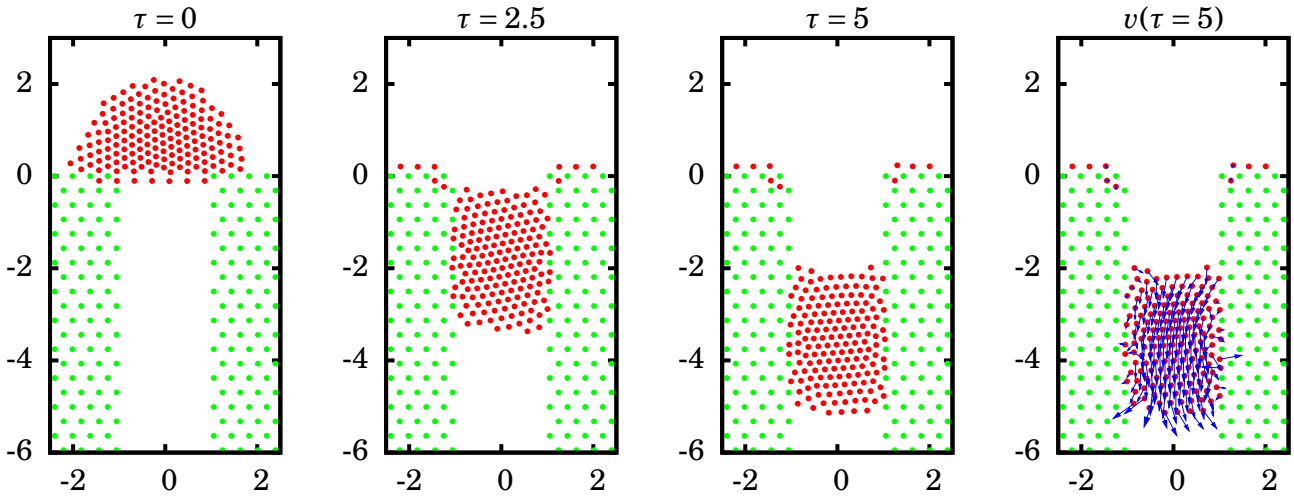

Figure 5.8: *Movement of water particles through a graphite capillary*

6 Conclusions

In this work quasi-molecular modelling of a water drop on a graphite surface was done following the model of D. Greenspan [15]. The model tries to preserve as much as possible microscopic characteristics without the massive amount of computation power needed for full Molecular Dynamics due to the great number of molecules. Pseudo-particles are introduced, which contain a large number of water particles. To describe the behaviour of these pseudo-particles on a macroscopic scale their interactions are calculated from Mie-potentials, which need to be determined for the system studied. Extra terms for surface tension can be avoided unlike in Navier-Stokes-fluid models, because this is already represented in the effective interaction potentials.

The derivation of the model was checked and compared with other references. The main problem of the implementation was the run-time problem as the calculations were computational costly. Therefore, efforts were invested to optimise the code to allow for shorter run-times. The results of the application of the model show that with certain parameter combinations some of the physical properties of water could be qualitatively fulfilled, like a correct contact angle with the surface. However, other physics properties were then incorrect, like the force holding the drop on the surface. This was then too strong compared with the gravitational force, preventing a realistic separation of the drop. The analytical analysis of the model showed that the equilibrium distance in the potential and the chosen cut-off distance are the only free parameters to be chosen. Therefore, the connection to additional microscopic properties like total internal energy as stated by the D. Greenspan is not really existing, limiting the physics model to rather qualitative effects.

In summary, the hybrid model delivers only qualitative results. It is not capable to be used for predictive, quantitative studies. Therefore, the challenge of building a realistic multi-scale model of water drops interacting with surfaces still remains.

References

[1] K. V. Beard, V. Bringi, and M. Thurai, "A new understanding of raindrop shape," *Atmospheric Research*, vol. In Press, Corrected Proof, pp. –, 2010.

[2] B. J. Mason, "Physics of a raindrop," *Physics Education*, vol. 13, no. 7, p. 414, 1978.

[3] P. Brunet, J. Eggers, and R. D. Deegan, "Vibration-induced climbing of drops," *Phys. Rev. Lett.*, vol. 99, p. 144501, Oct 2007.

[4] P. Brunet, J. Eggers, and R. D. Deegan, "Motion of a drop driven by substrate vibrations," *The European Physical Journal - Special Topics*, vol. 166, pp. 11–14, Jan 2009.

[5] X. Noblin, A. Buguin, and F. Brochard-Wyart, "Vibrations of sessile drops," *The European Physical Journal - Special Topics*, vol. 166, pp. 7–10, Jan 2009.

[6] P. Aussillous and D. Qu'er'e, "Liquid marbles," *Nature*, vol. 411, no. 6840, pp. 924–927, 2001.

[7] D. Richard and D. Quéré, "Viscous drops rolling on a tilted non-wettable solid," *EPL (Europhysics Letters)*, vol. 48, no. 3, p. 286, 1999.

[8] zastavki.com, july 2010. *http://www.zastavki.com/eng/Nature/Plants/wallpaper-8474.htm*.

[9] D. Greenspan, "Supercomputer simulation of liquid drop formation on a solid surface," *International Journal for Numerical Methods in Fluids*, vol. 13, pp. 895–906, Oct. 1991.

[10] M. J. P. Nijmeijer, C. Bruin, A. B. van Woerkom, A. F. Bakker, and J. M. J. van Leeuwen, "Molecular dynamics of the surface tension of a drop," *The Journal of Chemical Physics*, vol. 96, no. 1, pp. 565–576, 1992.

[11] S. M. Thompson, K. E. Gubbins, J. P. R. B. Walton, R. A. R. Chantry, and J. S. Rowlinson, "A molecular dynamics study of liquid drops," *The Journal of Chemical Physics*, vol. 81, no. 1, pp. 530–542, 1984.

[12] T. Jakubov and D. Mainwaring, "The surface tension of a solid at the solid-vacuum interface, an evaluation from adsorption and wall potential calculations," *Journal of colloid and interface science*, vol. 307, no. 2, pp. 477–480, 2007.

[13] XYdatasource.com, june 2010. *http://www.xydatasource.com/xy-showdatasetpage.php?dsid=107&datasetcode=4444*.

[14] T. Chow, "Wetting of rough surfaces," *Journal of Physics: Condensed Matter*, vol. 10, p. L445, 1998.

[15] D. Greenspan, "Quasimolecular simulation of large liquid drops," *Journal of Physics D: Applied Physics*, vol. 22, no. 9, p. 1415, 1989.

[16] M. S. Korlie, "Particle modeling of liquid drop formation on a solid surface in 3-d," *Computers & Mathematics with Applications*, vol. 33, no. 9, pp. 97 – 114, 1997.

[17] M. S. Korlie, "Three-dimensional computer simulation of liquid drop evaporation," *Computers & Mathematics with Applications*, vol. 39, no. 12, pp. 43 – 52, 2000.

[18] M. Mahmoudi, "Particle modelling of fluid phenomena in 3-d," *Computers & Mathematics with Applications*, vol. 20, no. 3, pp. 25 – 44, 1990.

[19] R. Edgeworth, B. Dalton, and T. Parnell, "The pitch drop experiment," *European Journal of Physics*, vol. 5, p. 198, 1984.

[20] F. Mourits and F. Rummens, "A critical evaluation of Lennard–Jones and Stockmayer potential parameters and of some correlation methods," *Canadian Journal of Chemistry*, vol. 55, no. 16, pp. 3007–3020, 1977.

[21] XYdatasource.com, june 2010. *http://www.xydatasource.com/xyshowdatasetpage.php?datasetcode=35484&dsid=111&searchtext=water*.

7 Acknowledgement

It is a pleasure to thank those who have made this thesis possible. First of all my supervisor Prof. Dr. Ralf Schneider for the idea, the extraordinary support, the many ideas and last but not least the constant coffee supply. Secondly, Robert Warmbier, Gunnar Stoppa and Lars Lewerentz for the support, guiding, the done corrections and given inspirations. Furthermore Tim Teichmann, who gave almost all the solutions for the uncounted small problems I was to lazy to think about. And I would also like to give my parents Volker Jansen and Katrin Nagel a special thanks.